Localizing the origin of focal atrial tachycardia by combining clinical characteristics with P-wave morphology

Yun-peng Qu, MD, Xiao-gang Guo, MD, Jian Ma, MD

From the State Key Laboratory of Cardiovascular Disease, Arrhythmia Center, Fuwai Hospital, National Center for Cardiovascular Diseases, Chinese Academy of Medical Sciences and Peking Union Medical College, Beijing, China.

BACKGROUND Analyzing the P-wave morphology of an electrocardiogram (ECG) may determine the origin of focal atrial tachycardia (AT), thereby providing information for mapping and ablation.

OBJECTIVE We sought to analyze the ECG and clinical characteristics of focal ATs with different origins and to improve the 2021 Kistler algorithm.

METHODS We included 226 focal AT patients treated with radiofrequency catheter ablation. The origin of AT was determined by intracardiac electrophysiological examination. The diagnostic value of the 2021 Kistler algorithm was evaluated. The ECG and clinical characteristics of frequently misidentified cases were compared with those of patients with AT originating from adjacent locations. The algorithm was then modified and re-evaluated.

RESULTS The sensitivity of the Kistler algorithm for the diagnosis of left atrial appendage (LAA), left pulmonary vein (LPV), and right atrial appendage origins was 62.5%, 61.1%, and 52.9%, respectively. An incessant attack was a common feature of atrial appendage origins ($P < .05$). Focal AT originating from the LPV was more likely to be accompanied by atrial fibrillation than one originating from the LAA ($P < .05$). The algorithm was modified based on these results. The sensitivity of the new algorithm for distinguishing origins in the LAA, LPV, and right atrial appendage was 75.0%, 61.1%, and 70.6%; the specificity was 95.0%, 96.6%, and 95.0%; and the accuracy was 94.2%, 93.8%, and 96.9%, respectively.

CONCLUSION The presence of atrial fibrillation and the incessancy of the attack can aid in distinguishing focal ATs originating from pulmonary veins and atrial appendages from those originating from adjacent locations.

KEYWORDS Electrocardiogram; P-wave morphology; Clinical features; Focal atrial tachycardia; Differential diagnosis algorithm

(Heart Rhythm O^2 2025;6:463–472)

Introduction

Among the types of supraventricular tachycardia, focal atrial tachycardia (AT) is relatively rare, accounting for approximately 7% of all cases.[1] The common origins of focal AT are the crista terminalis (CR), tricuspid annulus (TA), coronary sinus (CS) ostium and intramuscular sleeve, atrial septum and atrioventricular (AV) node region, right atrial appendage (RAA), pulmonary vein antrum and muscular sleeve, mitral annulus (MA), and left atrial appendage (LAA). In addition, focal AT can also originate from atypical locations, such as the superior vena cava (SVC). Successful ablation depends on accurate mapping, and analyzing the P-wave morphology of an electrocardiogram (ECG) at the onset of AT may determine the origin, thereby providing key information for mapping and ablation.

In 2006, Kistler and colleagues[2] reported a diagnostic algorithm based on P-wave morphology to determine the origin of focal AT. This algorithm was improved in 2021, and its accuracy was reported to be 93%.[3] However, it is difficult to provide an accurate assessment of the origin of focal AT by relying solely on ECG. Under certain clinical conditions, the P-wave is often hidden in the QRS complex or T-wave, complicating accurate identification. Uhm and colleagues[4] tried to integrate clinical characteristics, including the presence of atrial fibrillation and the frequency of onset, into the original algorithm to play an auxiliary role in origin identification. In this study, the P-wave of focal AT was accurately identified in a catheter laboratory, and the similarities and differences in P-wave morphology, as well as the clinical characteristics of patients, were analyzed. The aim of this study was to improve the 2021

Address reprint requests and correspondence: Dr Xiao-gang Guo, State Key Laboratory of Cardiovascular Disease, Arrhythmia Center, Fuwai Hospital, National Center for Cardiovascular Diseases, Chinese Academy of Medical Sciences and Peking Union Medical College, 100037 Beijing, China. E-mail address: laogang26@163.com.

2666-5018/

https://doi.org/10.1016/j.hroo.2025.01.012

KEY FINDINGS

- The diagnostic value of the 2021 Kistler algorithm was evaluated by revealing the P-wave through rapid ventricular pacing in catheter laboratories. The results indicate that the Kistler method still has room for improvement.
- The electrocardiogram and clinical characteristics of patients with focal atrial tachycardia originating from different locations were analyzed, and a combined localizing method was established on the basis of the results.
- The presence of atrial fibrillation and the incessancy of the attack can aid in distinguishing focal atrial tachycardias originating from pulmonary veins and atrial appendages from those originating from adjacent locations.

diagnostic algorithm of Kistler and colleagues and to establish a new set of diagnostic algorithms and evaluate their diagnostic value.

Methods

Study population

From February 2011 to April 2021, 270 patients with focal AT were admitted to Fuwai Hospital for cardiac electrophysiological examination and radiofrequency ablation. The specific inclusion criteria were as follows: (1) ECG or Holter monitoring revealed paroxysmal, incessant or sustained episodes of AT, and spontaneous or induced AT was observed during electrophysiological surgery with consistent P-wave morphologies; (2) focal AT was clearly diagnosed through intraoperative electrophysiological examination and mapping; (3) the morphology of AT P waves recorded outside the catheter laboratory had to match those recorded during mapping; and (4) the ablation effect in all cases should be definitive, with no AT inducible under isoproterenol infusion and programmed stimulation, and no AT recurrence reported during a follow-up period of at least 1 month. The exclusion criteria were as follows: (1) history of previous catheter ablation or Cox maze surgery to treat atrial fibrillation; (2) multifocal AT; or (3) incomplete or ineffective ablation, with AT recurring immediately or during hospitalization.

The inclusion criteria for specific groups were as follows: (1) patients with clinically premature atrial contraction in >50% of daily heartbeats or (2) patients with accelerated atrial rhythm and an atrial rate ranging between 60 and 120 beats/min. According to the previous inclusion and exclusion criteria, 226 patients with focal AT treated with radiofrequency catheter ablation at Fuwai Hospital from December 2013 to April 2021 were included in this study. Nine patients with multifocal AT and 35 patients with incomplete or ineffective ablation were excluded.

Definitions

AT was defined as more than 3 consecutive premature atrial beats with an atrial frequency of more than 100 beats/min, characterized by the presence of isoelectric lines between P waves in all leads, with activation spreading centrifugally from the earliest activation site during catheter electrogram mapping. Persistent AT was defined as episodes lasting more than 7 days that could not be corrected to sinus rhythm by medication or electrical cardioversion, or correction was not attempted. Incessant AT was defined as recurrent episodes and cessation of AT, with no more than 2 sinus rhythm beats between episodes or accounting for more than 90% of the total number of beats per day.[1]

Electrophysiological examination

The study was ethically approved by Fuwai Hospital, and all patients provided informed consent. The study also adhered to the Declaration of Helsinki. Class I and III antiarrhythmic drugs were stopped for at least 5 half-lives before surgery, and amiodarone was stopped for at least 3 weeks. All patients underwent electrophysiological interventional examination in a fasted, awake state. A multielectrode catheter (Biosense Webster) was placed at the recording sites of the electrogram of His bundle, CS, and right ventricular apex. A 12-lead body surface ECG and an intracardiac ECG at the previous positions were recorded synchronously with a multichannel physiological recorder (LabSystem Pro; Bard Medical). If premature atrial contraction or AT was absent, ventricular and atrial programmed stimulation and graded increasing stimulation were performed in succession. Patients in whom AT could not be induced by these stimuli were given an intravenous infusion of isoproterenol (up to 6 μg/min), and the stimulation procedure was repeated.

ECG data collection and interpretation

Because the P-wave, particularly the initial part of the wave, occasionally overlaps the T-wave and QRS complex, if a preoperative ECG recording the P-wave morphology at the onset of AT was not available, the following methods were used to expose the P-wave during spontaneous or induced AT in electrophysiological examinations: (1) a 12-lead ECG was used to record the P-wave morphology at the onset of AT when atrial activation was irregularly conducted to the ventricles; (2) Valsalva maneuvers were performed or drugs such as adenosine were administered to affect the conducting function of the AV node, slowing anterograde conduction and revealing the P-wave; or (3) the P-wave could be revealed when the ventricles were rapidly paced at a rate that could not maintain 1:1 reverse atrial conduction and pacing was terminated.

The recorded P waves were described in the following ways, regardless of the recording method: (1) positive (+), a positive deviation from the equipotential line; (2) negative (–), negative deviation from the equipotential line; (3) isoelectric potential, deviation from the isoelectric line no more than 0.05 mV; (4) bidirectional, positive-to-negative (+/–), a

positive followed by negative deviation from the equipotential line; and (5) bidirectional, negative-to-positive (–/+), negative followed by positive deviation from the equipotential line.

The morphology of the P-wave was categorized by 2 experienced electrocardiographic specialists individually, and the origin of the AT was determined according to the 2021 algorithm by Kistler and colleagues.[2] The 2 specialists were blinded to other clinical data or the mapping results. Any differences were resolved through communication and consensus between the 2 specialists. If no consensus was reached, a third ECG specialist analyzed the wave and gave the final result.

Mapping

A small subset (10 cases) was mapped solely with the assistance of x-ray imaging, but most cases were mapped with CARTO XP or CARTO 3 three-dimensional electroanatomic mapping systems (Biosense Webster). When a left atrial origin was suspected, a Brockenbrough atrial septal puncture needle was used to puncture the atrial septum, and an indwelling SL1 sheath (Medtronic) was used to establish a transseptal pathway for left atrial mapping. The origins were defined as follows[5]:

- CR: the longitudinal double-potential area from the right atrial free wall to the area between the SVC and RAA.[6]
- Left pulmonary vein (LPV)/right pulmonary vein (RPV): the antrum, ostium, and interior of the LPV/RPV with clear angiographical evidence.
- LAA/RAA: the area inside the LAA or RAA with clear angiographical evidence.[7–9]
- TA: the nonseptal annulus region, with a lower edge 1 cm away from the CS ostium and an upper edge 1 cm away from His bundle. When the ablation catheter is stable, a characteristic annulus motion is observed from the left anterior oblique or right anterior oblique perspective, and the proportion of locally recorded A/V potential amplitude is between 1:10 and 1:1 and the amplitude of the ventricular electrogram exceeds 0.5 mV.[10]
- Paraseptal: includes the atrial septum, AV node area, ostium of the CS, noncoronary aortic cusp, and high MA. These origins have very similar anatomic locations and ECG performance, increasing the difficulty in distinguishing them, so Kistler and colleagues combined these regions into the "paraseptal" origin. Each location is defined as follows[11–15]:
  - Atrial septum: oval fossa area and primary atrial septum.
  - AV node area: within 1 cm of the recording location of the proximal bundle of His, including the Koch triangle and aortic MA junction area.
  - CS ostium: the area where the earliest atrial potential was recorded at the proximal end of the CS electrode and the successful ablation target was located within 1 cm from the ostium of the CS.
  - Noncoronary aortic cusp: the area from the left anterior oblique or right anterior oblique perspective in which proximal aorta angiography revealed that the ablation catheter was located in the noncoronary aortic cusp, and the local bipolar electrogram showed a large A-wave.[12]
  - High MA: from the left anterior oblique or right anterior oblique perspective with a stable ablation catheter, a characteristic annulus motion is observed, with the catheter and CS electrode moving synchronously in the same direction. The proportion of locally recorded A/V potential amplitude is between 1:10 and 1:1, and the amplitude of the ventricular electrogram exceeds 0.5 mV.
  - Other locations: rare origins that can include the SVC; right atrial free wall and posterior wall; left atrial posterior wall, apical wall, and anterior wall; mitral isthmus; and the proximal middle cardiac vein.[16]

Radiofrequency catheter ablation and other treatments

Point ablation was first attempted. If the origin could not be successfully ablated, circular ablation was performed to block abnormal electrical activity from entering the atrium. Saline perfusion catheters (Navistar; Biosense Webster) were used at 43 °C, 30 W, and 17 mL/min, whereas nonsaline perfusion catheters were used with a power of 30 W and no temperature control. The ablation of origins in the AV node region, especially those adjacent to the His bundle region, and inside the CS used a starting power of 15 W that was gradually titrated up to a maximum of 30 W. After the ablation procedure, induction of AT by repeated stimuli with isoproterenol infusion was attempted. A successful endpoint was the termination of AT by ablation, with no spontaneous or inducible AT recurrence after the operation.[1]

Statistical analysis

Continuous variables are expressed as the mean ± SD or medians and ranges, and count data are expressed as count and percentage. The Wilcoxon nonparametric test was used for comparisons between 2 groups. A 2-sided P value $<.05$ was considered statistically significant. In the differential diagnosis, for each kind of focal AT originating from a specific location, correctly diagnosed cases were defined as true positives, nonexcluded cases at other locations were defined as false positives, correctly excluded cases at other locations were defined as true negatives, and nondiagnosed cases at the specified location were defined as false negatives. Statistical analyses were performed using IBM SPSS statistics 26.0 software.

Results

Baseline data

A total of 226 cases of focal AT were included in this study. The ECG data of 137 (60.6%) cases were collected before the catheter ablation procedure, while that of the remaining 89 (39.4%) cases were recorded in a catheter laboratory. The distribution of the baseline clinical data of the patients in each group according to the origin of the focal AT is shown in

Table 1 Baseline clinical data

Origin (cases)	CR (n = 19)	LPV (n = 18)	RPV (n = 36)	LAA (n = 8)	RAA (n = 17)	TA (n = 27)	MA (n = 7)	Septum (n = 13)	AV node (n = 7)	CS ostium (n = 29)	NCC (n = 22)	SVC (n = 8)	RAPW (n = 7)	LAPW (n = 6)	LAAW (n = 2)
Male/female	5/14	8/10	21/15	4/4	7/10	15/12	5/2	7/6	1/6	20/9	6/16	5/3	3/4	3/3	0/2
Age, y	52.1 ± 15.4	36.8 ± 17.6	43.8 ± 17.0	28.1 ± 19.9	38.3 ± 22.6	52.7 ± 17.6	32.6 ± 14.7	40.9 ± 23.7	52.4 ± 11.4	41.9 ± 16.4	58.2 ± 13.0	56.5 ± 19.4	50.0 ± 14.3	50.2 ± 13.7	48.5 ± 0.7
History, y	5.1 ± 4.7	4.3 ± 3.2	6.9 ± 5.3	4.1 ± 5.5	4.9 ± 6.2	6.2 ± 7.6	3.1 ± 2.1	3.0 ± 2.1	6.6 ± 3.9	4.6 ± 3.9	8.0 ± 7.3	8.1 ± 5.1	7.3 ± 8.8	4.3 ± 6.2	7.5 ± 3.5
Hypertension	7 (37)	2 (11)	10 (28)	1 (13)	3 (18)	6 (22)	1 (14)	1 (8)	1 (14)	8 (28)	10 (45)	1 (13)	3 (43)	1 (17)	1 (50)
Diabetes	0 (0)	2 (11)	2 (6)	0 (0)	1 (6)	2 (7)	1 (14)	2 (15)	0 (0)	2 (7)	6 (27)	0 (0)	1 (14)	0 (0)	0 (0)
CHD	0 (0)	0 (0)	4 (11)	0 (0)	0 (0)	5 (19)	0 (0)	0 (0)	0 (0)	1 (3)	4 (18)	2 (25)	0 (0)	0 (0)	0 (0)
SHD	1 (5)	0 (0)	2 (6)	1 (13)	4 (24)	1 (4)	0 (0)	1 (8)	1 (14)	1 (3)	0 (0)	0 (0)	1 (14)	1 (17)	0 (0)
PAF	0 (0)	8 (44)	9 (25)	0 (0)	0 (0)	0 (0)	0 (0)	0 (0)	3 (43)	0 (0)	0 (0)	0 (0)	0 (0)	0 (0)	0 (0)
Palpitation	19 (100)	18 (100)	36 (100)	7 (88)	16 (94)	25 (93)	7 (100)	13 (100)	7 (100)	29 (100)	22 (100)	8 (100)	7 (100)	6 (100)	2 (100)
Syncope	0 (0)	0 (0)	1 (3)	1 (13)	0 (0)	0 (0)	0 (0)	1 (8)	0 (0)	2 (7)	1 (5)	1 (13)	0 (0)	0 (0)	0 (0)
Incessancy	2 (11)	0 (0)	1 (3)	4 (50)	11 (65)	1 (4)	0 (0)	0 (0)	0 (0)	3 (10)	5 (23)	2 (25)	5 (71)	0 (0)	0 (0)
AAD(s)	1.1 ± 0.7	0.8 ± 0.8	0.8 ± 0.7	0.8 ± 0.9	0.8 ± 0.8	0.7 ± 0.7	0.6 ± 0.8	0.6 ± 0.7	0.9 ± 0.9	0.7 ± 0.7	0.8 ± 0.7	1.5 ± 0.5	1.0 ± 1.0	1.2 ± 1.0	0.5 ± 0.7
Amiodarone	3 (16)	4 (22)	5 (14)	0 (0)	2 (12)	2 (7)	0 (0)	2 (15)	1 (14)	4 (14)	2 (9)	4 (50)	0 (0)	1 (17)	0 (0)
LAEDD, mm	32.7 ± 4.4	33.4 ± 2.1	32.9 ± 4.6	35.0 ± 6.0	33.4 ± 6.8	35.3 ± 4.2	34.7 ± 3.0	34.8 ± 3.0	31.7 ± 6.1	34.0 ± 4.6	33.8 ± 4.2	37.4 ± 6.3	34.1 ± 4.0	38.2 ± 1.9	35.5 ± 7.8
LVEDD, mm	42.9 ± 4.6	45.8 ± 3.1	45.2 ± 3.3	50.0 ± 6.8	47.2 ± 7.8	47.6 ± 4.4	46.1 ± 3.9	45.2 ± 3.1	45.0 ± 4.4	45.3 ± 4.7	44.3 ± 3.4	46.4 ± 5.2	46.1 ± 5.5	50.3 ± 2.6	49.0 ± 2.8
LVEF, %	63.3 ± 6.2	62.5 ± 5.6	63.6 ± 4.5	54.9 ± 16.8	56.2 ± 13.0	63.4 ± 5.5	60.6 ± 5.8	62.8 ± 5.5	62.7 ± 7.3	60.9 ± 5.2	64.0 ± 5.0	63.1 ± 4.2	65.0 ± 5.8	64.2 ± 3.4	64.5 ± 3.5
TCL, ms	377.1 ± 77.1	388.6 ± 76.1	390.8 ± 67.7	400.5 ± 47.3	416.4 ± 56.0	410.2 ± 66.0	386.3 ± 68.6	402.2 ± 70.0	369.1 ± 30.2	385.3 ± 78.3	391.1 ± 56.0	386.0 ± 81.0	397.4 ± 85.4	390.0 ± 94.5	396.0 ± 45.3

Values are n, mean ± SD, or n ().

AAD = antiarrhythmic drug; AV node = atrioventricular node; CHD = coronary heart disease; CR = crista terminalis; CS = coronary sinus; LAA = left atrial appendage; LAAW = left atrial anterior wall; LAEDD = left atrial end-diastolic diameter; LAPW = left atrial posterior wall; LPV = left pulmonary vein; LVEDD = left ventricular end-diastolic diameter; LVEF = left ventricular ejection fraction; MA = mitral annulus; NCC = noncoronary aortic cusp; PAF = paroxysmal atrial fibrillation; RAA = right atrial appendage; RAPW = right atrial posterior wall; RPV = right pulmonary vein; SHD = structural heart disease; SVC = superior vena cava; TA = tricuspid annulus; TCL = tachycardia cycle length.

Table 1, and the distribution of the origins is shown in Figure 1.

Effectiveness of the current algorithm

The improved differential diagnosis algorithm reported by Kistler and colleagues[2] in 2021 was used to identify the origin of 226 cases of focal AT. A total of 151 cases were correctly identified. The overall accuracy rate was 66.8%. However, this algorithm did not include rare sites of origin. If these cases are excluded, the overall accuracy rate is 77.0%. For each origin, the diagnostic value of the 2021 Kistler algorithm is shown in Table 2.

The sensitivity of the Kistler algorithm for the diagnosis of origins in the RAA, LAA, and LPV was 52.9%, 62.5%, and 61.1%, respectively, which was lower than the sensitivity for the other locations. Moreover, Kistler attributed the LAA and LPV to 1 set of diagnostic processes and the TA and RAA to another set of diagnostic processes. This "fuzzy" processing method improves the effectiveness of the algorithm, but there is still room for improvement. With the current algorithm, most of the unidentified cases of LAA or LPV origin were categorized as having a CR or RPV origin. The critical issue in missed diagnoses was identifying the bifid P-wave in lead II/V_1. Most of the unidentified cases of RAA origin were categorized as having a TA origin, and a small proportion were categorized as having a CR origin. The critical issues in missed diagnoses were identifying the nonpositive P-wave in leads V_2 to V_4 and the non-negative P-wave in leads II, III, and aVF. The results of the analysis of the false negative case diagnoses are shown in Table 3.

Improvement of the current algorithm

The low sensitivity of the current algorithm for diagnosing the LPV/LAA origin is related to the high dependence on identifying bifid P waves in lead II or lead V_1, and the low sensitivity for the RAA origin is related to the inability to distinguish between the RAA, CR, and TA origins effectively. Therefore, the improvement of this algorithm mainly focuses on the establishment of a differential diagnostic process for LPV/LAA origins that does not overly rely on bifid P waves and the effective differentiation of RAA, CR, and TA origins.

The clinical and ECG characteristics of focal ATs originating from LPV vs LAA, RAA vs CR, and RAA vs TA are shown in Tables 4 and 5. In terms of clinical characteristics, persistent or incessant attack is a common characteristic of focal AT originating from atrial appendages and is significantly different from AT of other origins ($P < .05$). Compared with AT originating from the LAA, focal AT originating from the LPV was more likely to be associated with atrial fibrillation ($P < .05$). In terms of the ECG findings, the P-wave of focal AT originating from the CR usually moves upward in earlier leads ($P < .001$), whereas there is no significant difference in the P waves of focal ATs between the RAA and TA and between the LAA and LPV.

The algorithm was modified based on the results of this study. Using onset characteristics and accompanying

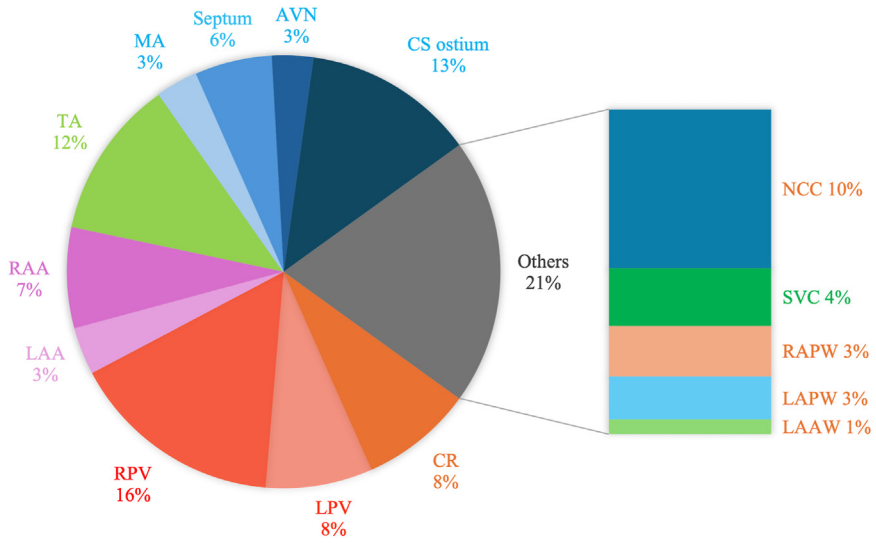

Figure 1 The distribution of the origins. Different sections in the pie chart show the proportion of focal atrial tachycardia with different origins in all enrolled cases. AVN = atrioventricular node; CR = crista terminalis; CS = coronary sinus; LAA = left atrial appendage; LAAW = left atrial anterior wall; LAPW = left atrial posterior wall; LPV = left pulmonary vein; MA = mitral annulus; NCC = noncoronary aortic cusp; RAA = right atrial appendage; RAPW = right atrial posterior wall; RPV = right pulmonary vein; SVC = superior vena cava; TA = tricuspid annulus.

diseases, cases with origins in the RAA and LAA were further differentiated from cases with TA/RAA origins and LPV/LAA origins as determined by the Kistler algorithm. In addition, a new method to determine the LAA origin independent of the bifid P-wave in lead II/V_1 was added. The new algorithm was used to differentially diagnose the enrolled patients, and the results are shown in Table 6. The new process, as shown in Figure 2, distinguished the gray areas in the Kistler algorithm to a certain extent while achieving better sensitivity, specificity, and accuracy. Figure 3 shows an example of focal AT originating from LAA, whose diagnosis was improved form the Kistler algorithm.

Discussion

Limitations and significance of ECG diagnosis

Owing to its convenient, noninvasive, and cost-effective nature, ECG examination is often used as the main data source for electrophysiologists in clinical practice. However, it still has considerable limitations in the diagnosis of focal AT.

On the one hand, the diagnosis of the origin of AT is highly dependent on the interpretation of P-wave morphology, while the P-wave is often overlapped by the previous T-wave even when the image quality is relatively high. In a previous study by Uhm and colleagues,[4] analysis failed in 32% of cases because of the lack of identifiable P waves. With the help of drugs to reduce AV transmission, Tang and colleagues[17] successfully recorded the P waves of all 31 patients in their study. In this study, P waves could be recorded in only 137 of 226 cases without utilizing a catheter laboratory, and medication was usually needed to control the ventricular rate. Therefore, it is challenging to obtain a clear and distinguishable P-wave.

On the other hand, because P waves originating from adjacent locations can be very similar, even if identifiable P waves are collected, the origin of AT can often be

Table 2 The diagnostic value of the 2021 Kistler algorithm Values are n, unless otherwise indicated

Origin (cases)	CR (n = 19)	LPV (n = 18)	RPV (n = 36)	LAA (n = 8)	RAA (n = 17)	TA (n = 27)	Paraseptal (n = 78)
True positive	14	11	32	5	9	21	58
False positive	27	6	34	6	3	7	17
True negative	180	202	156	212	206	192	131
False negative	5	7	4	3	8	6	20
Sensitivity, %	73.7	61.1	88.9	62.5	52.9	77.8	74.4
Specificity, %	86.9	97.1	82.1	97.2	98.6	96.5	88.5
Accuracy, %	85.8	94.2	83.2	96.0	95.1	94.2	83.6
PPV, %	34.1	64.7	48.5	45.5	75.0	75.0	77.3
NPV, %	97.3	96.7	97.5	98.6	96.3	97.0	86.8

CR = crista terminalis; LAA = left atrial appendage; LPV = left pulmonary vein; NPV = negative predictive value; PPV = positive predictive value; RAA = right atrial appendage; RPV = right pulmonary vein; TA = tricuspid annulus.

Table 3 Issues and corresponding cases in misidentified origins

Issues	V_1+	II/V_1 bifid	I–/isoelectric potential	V_1–	V_2–V_4 nonpositive	Inferior leads nonnegative
LPV (n = 7)	1 (14)	7 (71)	2 (29)	N/A	N/A	N/A
LAA (n = 3)	0	3 (100)	0	N/A	N/A	N/A
RAA (n = 8)	N/A	N/A	N/A	1 (13)	4 (50)	4 (50)

Values are n (%).

LAA = left atrial appendage; LPV = left pulmonary vein; N/A = not applicable; RAA = right atrial appendage.

misdiagnosed. Man and colleagues[18] reported that the anatomical resolution of P-wave localization through ECG was only 17 mm. In addition, when the patient's atrium exhibits anatomical variation or is affected by lesions, scars, or other factors, the relationship between P-wave morphology and the origin of the focal AT may be very different.[5,19] In conclusion, P-wave morphology and the origin of AT do not have a one-to-one correspondence. Distinguishing the origin of AT through analysis of the P-wave alone can be very difficult.

In this study, the P-wave was clearly revealed by rapid ventricular pacing in catheter laboratories to ensure that all enrolled patients could be analyzed.

Direction of improvement

The original Kistler algorithm did not distinguish LPV origins from LAA, high TA, RAA and other adjacent origins; instead, the ECG morphology of these adjacent origins was diagnosed as "both were possible," which was essentially a "fuzzy" processing method.[2] Kistler and colleagues[3] improved this algorithm in 2021, using the isoelectric or negative morphology of the P-wave in lead I to distinguish AT originating from the left and right sides of the left atrium and classifying origins in the CS ostium, atrial septum, AV node, noncoronary aortic cusp, and high MA as "paraseptal," which was still ambiguous. This processing method regressed the final significance of analyzing P-wave morphology and objectively improved the accuracy of the diagnostic process. However, Uhm and colleagues[4] attempted to distinguish the LAA from the left superior pulmonary vein and the SVC from the right superior pulmonary vein and other adjacent origins using analysis of P-wave morphology combined with clinical characteristics and reported that this method achieved satisfactory accuracy. This finding suggests that after taking the clinical characteristics of patients into consideration, there is still room for further improvement in Kistler's algorithm. The goal of improvement was to address the shortcomings of the process in terms of identification, ensure considerable diagnostic value, and reduce the gray areas in the algorithm as much as possible.

Identification of adjacent origins

According to the Kistler algorithm, patients without bifid P waves were directly classified as having non-LPV/LAA origins. Therefore, it was necessary to explore a diagnostic

Table 4 The clinical characteristics of focal ATs of easily misidentified origins

Origin (cases)	LPV (n = 18)	LAA (n = 8)	*P*	CR (n = 19)	RAA (n = 17)	*P*	TA (n = 27)	RAA (n = 17)	*P*
Male/female	8/10	4/4	.604	5/14	7/10	.489	15/12	7/10	.359
Age, y	36.8 ± 17.6	28.1 ± 19.9	.191	52.1 ± 15.4	38.3 ± 22.6	.129	52.7 ± 17.6	38.3 ± 22.6	.032
History, y	4.3 ± 3.2	4.1 ± 5.5	.385	5.1 ± 4.7	4.9 ± 6.2	.337	6.2 ± 7.6	4.9 ± 6.2	.595
Hypertension	2 (11)	1 (13)	.920	7 (37)	3 (18)	.151	6 (22)	3 (18)	.717
Diabetes	2 (11)	0 (0)	.336	0 (0)	1 (6)	.759	2 (7)	1 (6)	.847
CHD	0 (0)	0 (0)	1.000	0 (0)	0 (0)	1.000	5 (19)	0 (0)	.062
SHD	0 (0)	1 (13)	.134	1 (5)	4 (24)	.163	1 (4)	4 (24)	.046
PAF	8 (44)	0 (0)	.026	0 (0)	0 (0)	1.000	0 (0)	0 (0)	1.000
Palpitation	18 (100)	7 (88)	.134	19 (100)	16 (94)	.216	25 (93)	16 (94)	.847
Syncope	0 (0)	1 (13)	.134	0 (0)	0 (0)	1.000	0 (0)	0 (0)	1.000
Incessancy	0 (0)	4 (50)	.001	2 (11)	11 (65)	.015	1 (4)	11 (65)	.001
AAD(s)	0.8 ± 0.8	0.8 ± 0.9	.905	1.1 ± 0.7	0.8 ± 0.8	.289	0.7 ± 0.7	0.8 ± 0.8	.675
Amiodarone	4 (22)	0 (0)	.155	3 (16)	2 (12)	.982	2 (7)	2 (12)	.628
LAEDD, mm	33.4 ± 2.1	35.0 ± 6.0	.325	32.7 ± 4.4	33.4 ± 6.8	.813	35.3 ± 4.2	33.4 ± 6.8	.125
LVEDD, mm	45.8 ± 3.1	5.0 ± 6.8	.111	42.9 ± 4.6	47.2 ± 7.8	.212	47.6 ± 4.4	47.2 ± 7.8	.265
LVEF, %	62.5 ± 5.6	54.9 ± 16.8	.302	63.3 ± 6.2	56.2 ± 13.0	.021	63.4 ± 5.5	56.2 ± 13.0	.076
TCL, ms	388.6 ± 76.1	400.5 ± 47.3	.505	377.1 ± 77.1	416.4 ± 56.0	.117	410.2 ± 66.0	416.4 ± 56.0	.952

Values are n, mean ± SD, or n (%).

AAD = antiarrhythmic drug; AT = atrial tachycardia; CHD = coronary heart disease; CR = crista terminalis; LAA = left atrial appendage; LAEDD = left atrial end-diastolic diameter; LPV = left pulmonary vein; LVEDD = left ventricular end-diastolic diameter; LVEF = left ventricular ejection fraction; PAF = paroxysmal atrial fibrillation; RAA = right atrial appendage; SHD = structural heart disease; TA = tricuspid annulus; TCL = tachycardia cycle length.

Table 5 The ECG characteristics of focal ATs of easily misidentified origins

Lead/PWM	V_1					V_2-V_4				I				II/III/aVF				V_1 (SR)				II/V_1 bifid
	+	−	Isoelectric	+/−	−/+	+	−	Isoelectric potential	+/−	−/+	+	−	Isoelectric potential	+/−	−/+	+	−	Isoelectric potential	+/−	−/+	
LPV	17	1	0	0	0	15	0	2	1	0	1	3	13	0	1	15	0	3	0	0	6	6	6	0	0	11
LAA	8	0	0	0	0	4	0	4	0	0	0	4	4	0	0	8	0	0	0	0	6	1	1	0	0	5
P	.505					.114					.185					.229					.073					.947
CR	11	6	3	5	1	22	2	2	0	0	9	0	17	0	0	16	2	7	0	1	16	4	2	4	0	0
RAA	1	15	1	0	0	4	3	8	1	1	5	2	10	0	0	9	4	3	0	1	9	2	3	3	0	0
P			.728					<.001					.872					.801					.540			1.000
TA	1	23	1	0	2	3	8	12	1	3	13	0	14	0	0	6	15	5	0	1	11	4	6	6	0	0
RAA	1	15	1	0	0	4	3	8	1	1	5	2	10	0	0	9	4	3	0	1	9	2	3	3	0	0
P	.492					.654					.426					.184					.474					1.000

Values are n.

AT = atrial tachycardia; CR = crista terminalis; ECG = electrocardiogram; LAA = left atrial appendage; LPV = left pulmonary vein; PWM = P-wave morphology; RAA = right atrial appendage; SR = sinus rhythm; TA = tricuspid annulus.

process for LPV/LAA origins that did not overly rely on bifid P waves. Uhm and colleagues[4] reported that LAA origins could be identified by incessant or persistent attacks, and LPV origins could be identified by concomitant atrial fibrillation; nonincessant cases without atrial fibrillation could also be identified as having an LAA origin. However, Uhm and colleagues' study focused on the diagnosis of LPV AT and included more patients with LPV AT with atrial fibrillation (22 of 24 cases). Among the patients included in this study, only 44% of the patients with focal AT originating from the LPV were accompanied by atrial fibrillation, suggesting that if atrial fibrillation was used as the standard indicator to distinguish between LPV and LAA origins, more than half of cases with an LPV origin would be misjudged as having an LAA origin. The proportion of AT cases with incessant attacks was much greater for patients with an atrial appendage origin than for other origins, suggesting that some cases with LAA origins can be corrected from a misdiagnosis of CR/RPV origins. However, the specificity for the diagnosis of atrial appendage origins using incessant or persistent attacks is strong, but the sensitivity is still low. Among the patients with LAA AT included in this study, only half had the characteristics of incessant or persistent attacks. Therefore, relying on clinical characteristics could increase the differentiation of LPV/LAA AT, but they were not sufficient to completely separate LPV and LAA origins, and there was still a "gray area."

Most of the misdiagnosed cases of an RAA origin were classified as having a TA origin, and some cases were classified as having a CR or other origin. Anatomically, the RAA is a blind end located at the upper posterior part of the right atrium, which is more posterior and superior than the TA. The electrical activity originating in the RAA may show heterogeneous conduction when transmitted into the atrium.[7,8] Given these anatomical characteristics, theoretically, the electrocardiographic P-wave of focal AT originating from the RAA may manifest as follows: (1) the polarity of the P-wave in leads V_2 to V_4 is different from that of focal AT originating from the TA; (2) the proportion of positive P waves in leads II, III, and AVF is greater than that of focal AT originating from the TA; and (3) bifid P waves appear more easily in the right chest leads, such as lead V_1. However, there was no significant difference in the ECG performance between the TA and RAA patients included in this study, and the RAA group did not exhibit the previous characteristics. In the CR group, the precordial P-wave usually has an early transition to be positive, but this indicator was already included in the current Kistler algorithm. Therefore, distinguishing an RAA origin from adjacent origins by ECG alone is difficult. However, in terms of clinical characteristics, focal AT originating from the RAA tends to result in incessant or persistent attacks, which was significantly different from TA AT and CR AT. This feature could be used to screen for RAA AT. Notably, similar to the LAA origin, not all RAA AT cases have this indicator. Therefore, there was also a gray area in the diagnosis of TA/RAA AT. For patients whose ECG performance resulted in a diagnosis in this gray area,

Table 6 The diagnostic value of the modified algorithm

Origin (cases)	CR (n = 19)	LPV (n = 18)	RPV (n = 36)	LAA (n = 8)	RAA (n = 17)	TA (n = 27)	Paraseptal (n = 78)
True positive	16	11	31	6	12	21	58
False positive	21	7	29	11	2	4	17
True negative	186	201	161	207	207	195	131
False negative	3	7	5	2	5	6	20
Sensitivity, %	84.2	61.1	86.1	75.0	70.6	77.8	74.4
Specificity, %	89.9	96.6	84.7	95.0	99.0	98.0	88.5
Accuracy, %	89.3	93.8	85.0	94.2	96.9	95.6	83.6
PPV, %	43.2	61.1	51.7	35.2	85.7	84.0	77.3
NPV, %	98.4	96.6	97.0	99.0	97.6	97.0	86.8

Values are n, unless otherwise indicated.

CR = crista terminalis; LAA = left atrial appendage; LPV = left pulmonary vein; NPV = negative predictive value; PPV = positive predictive value; RAA = right atrial appendage; RPV = right pulmonary vein; TA = tricuspid annulus.

it was still necessary to repeatedly map and confirm an origin in adjacent locations in clinical practice.

The Kistler algorithm did not include the SVC or other rare locations as possible origins. Uhm and colleagues[4] reported that SVC AT can be identified by the characteristics of bifid P waves in lead V_1; however, this study did not find a reliable way to differentiate SVC AT, and meaningful statistics were difficult to obtain for other cases of rare origin because of the small sample size. Therefore, the new diagnostic algorithm still did not include the SVC or other rare foci of origin. The electrocardiographic characteristics, clinical manifestations, and possible differential diagnosis of focal AT originating from these locations still need to be clarified by further research.

Remaining limitations

This study still had considerable shortcomings and limitations. The sample size was still insufficient, especially for patients with atrial appendix origins, resulting in the possible missing of some potential entry points for differential diagnosis. Owing to the same reason, the available differential diagnosis methods for rare cases could not be summarized. The new algorithm was also unable to prospectively predict a new group of patients, and its diagnostic value could not

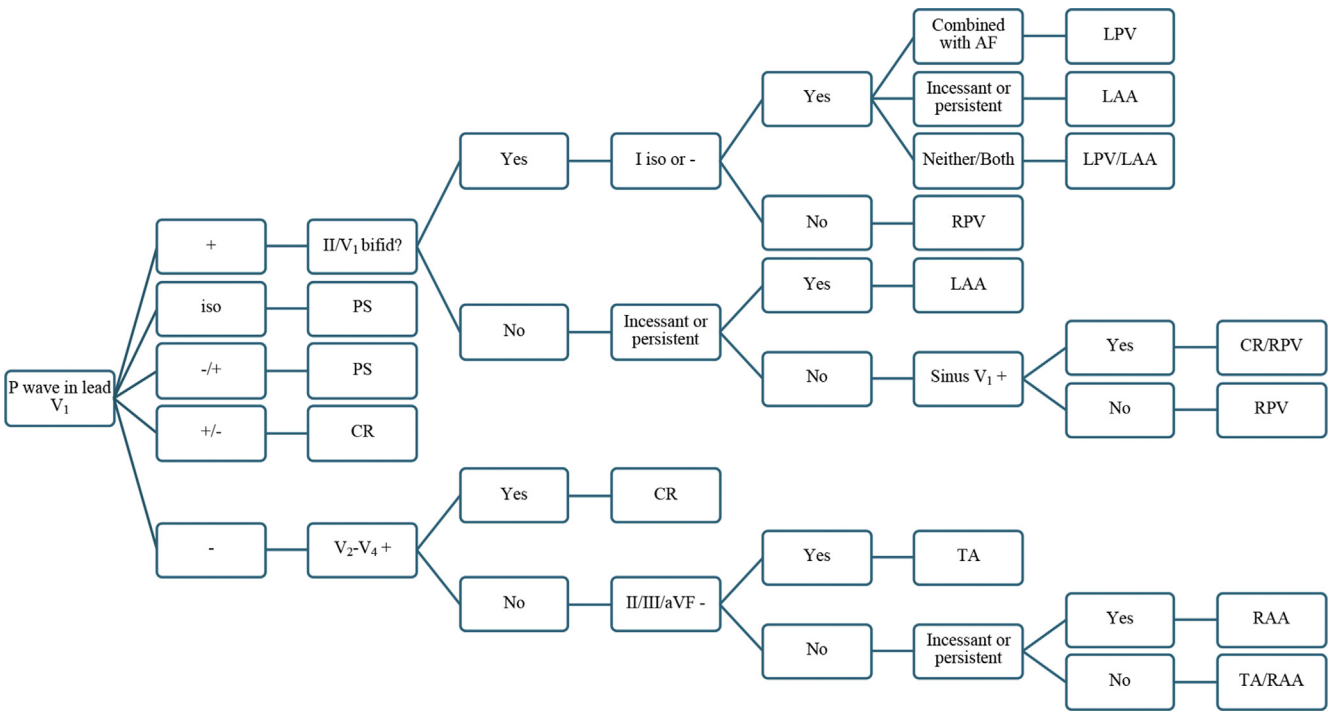

Figure 2 The new differential diagnosis algorithm combining clinical characteristics with P-wave morphology. + = positive; – = negative; iso = isoelectric potential; +/– = bidirectional, positive to negative; –/+ = bidirectional, negative to positive; AF = atrial fibrillation; CR = crista terminalis; LAA = left atrial appendage; LPV = left pulmonary vein; PS = paraseptal; RAA = right atrial appendage; RPV = right pulmonary vein; TA = tricuspid annulus.

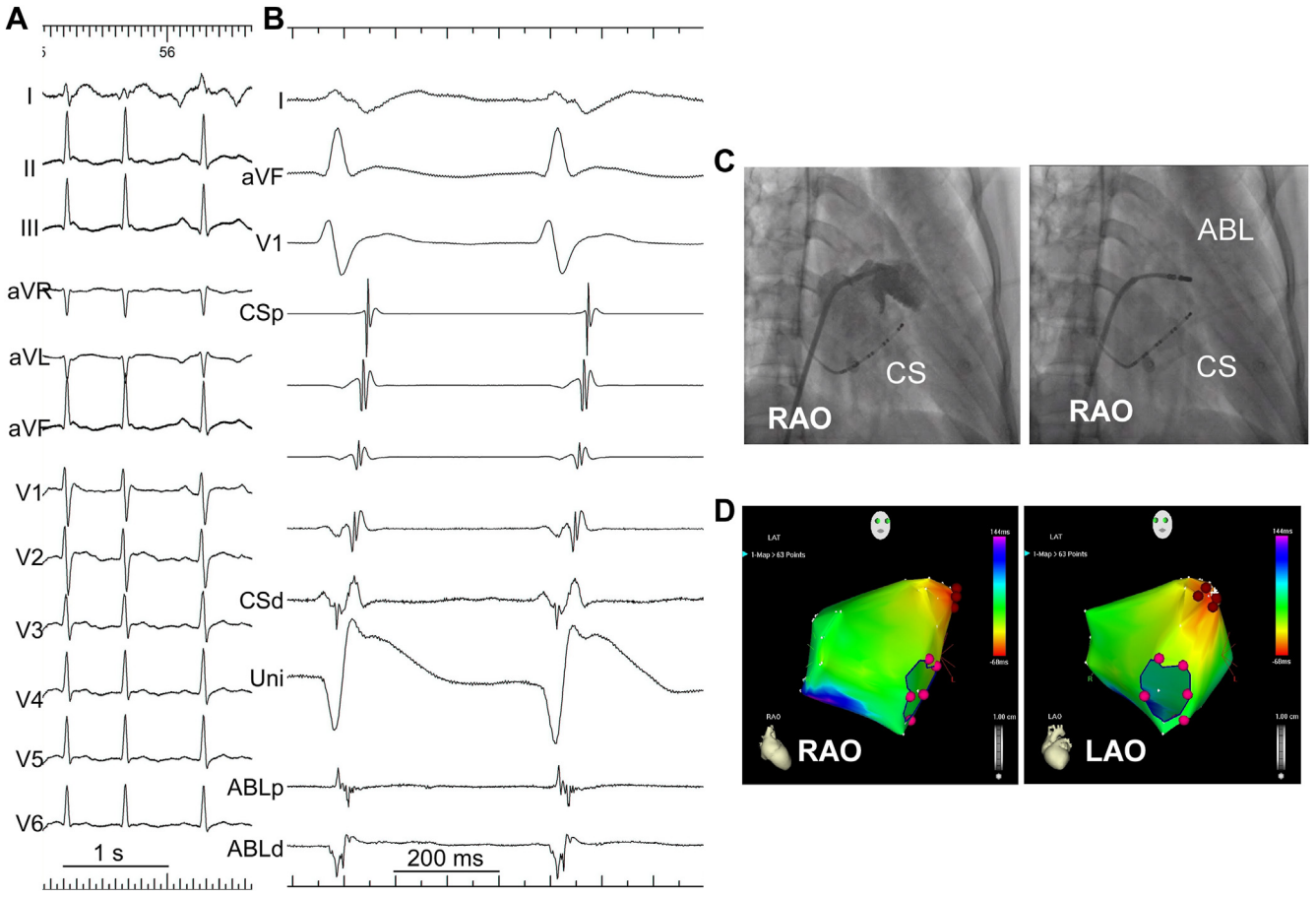

Figure 3 An example of focal atrial tachycardia originating from the left atrial appendage (LAA). Note that bifid P waves are absent in lead II or V_1, and the incessancy of the attack reveals the true origin. A: 12-lead electrocardiogram. B: Intracardiac electrogram at the ablation target. C: LAA angiogram and the location of the successful ablation target. Comparing the angiographic LAA contour, the successful ablation target is located at the apex of the LAA. D: Electroanatomic mapping. Red indicates the earliest activation and purple represents the latest activation, with the timing differences represented by a rainbow gradient. The red dot marks the successful ablation site, located at the apex of the LAA. ABLd = distal ablation catheter; ABLp = proximal ablation catheter; CSd = distal coronary sinus electrode; CSp = proximal coronary sinus electrode; LAO = left anterior oblique; RAO = right anterior oblique; Uni = unipolar electrogram.

be further evaluated. Second, as our hospital is a large electrophysiological center, a considerable number of the collected cases were transferred from other hospitals after ablation failure, so there was a selection bias. Future studies should include more cases of AT with different origins, especially rare origins, and focus on prospective predictions and possible corrections.

Conclusion

The combination of ECG P-wave morphology and clinical characteristics, including the presence of atrial fibrillation and the incessancy or persistency of the attack, can aid in distinguishing focal AT originating from the LAA and RAA from those originating from adjacent anatomical locations.

Funding Sources: This work was supported by a grant from National Natural Science Foundation of China (#82070351).

Disclosures: The authors have no conflicts to disclose.

Authorship: All authors attest they meet the current ICMJE criteria for authorship.

Patient Consent: The patients/participants provided written informed consent to participate in this study.

Ethics Statement: The studies involving human participants were reviewed and approved by Fuwai Hospital. The study also adhered to the Declaration of Helsinki.

References

1. Roberts-Thomson KC, Kistler PM, Kalman JM. Focal atrial tachycardia II: management. Pacing Clin Electrophysiol 2006;29:769–778.
2. Kistler PM, Roberts-Thomson KC, Haqqani HM, et al. P-wave morphology in focal atrial tachycardia: development of an algorithm to predict the anatomic site of origin. J Am Coll Cardiol 2006;48:1010–1017.
3. Kistler PM, Chieng D, Tonchev IR, et al. P-wave morphology in focal atrial tachycardia: an updated algorithm to predict site of origin. JACC Clin Electrophysiol 2021;7:1547–1556.
4. Uhm JS, Shim J, Wi J, et al. An electrocardiography algorithm combined with clinical features could localize the origins of focal atrial tachycardias in adjacent structures. Europace 2014;16:1061–1068.
5. Sánchez-Quintana D, Doblado-Calatrava M, Cabrera JA, et al. Anatomical basis for the cardiac interventional electrophysiologist. Biomed Res Int 2015;2015:547364.
6. Morris GM, Segan L, Wong G, et al. Atrial tachycardia arising from the crista terminalis, detailed electrophysiological features and long-term ablation outcomes. JACC Clin Electrophysiol 2019;5:448–458.

7. Yamada T, Murakami Y, Yoshida Y, et al. Electrophysiologic and electrocardiographic characteristics and radiofrequency catheter ablation of focal atrial tachycardia originating from the left atrial appendage. Heart Rhythm 2007; 4:1284–1291.
8. Zhang T, Li XB, Wang YL, et al. Focal atrial tachycardia arising from the right atrial appendage: electrophysiologic and electrocardiographic characteristics and catheter ablation. Int J Clin Pract 2009;63:417–424.
9. Narumi T, Naruse Y, Isogaki T, et al. Focal atrial tachycardia originating in the distal portion of the right atrial appendage aneurysm. Heart Rhythm 2022; 19:1217–1218.
10. Sato H, Yagi T, Namekawa A, et al. Focal atrial tachycardia arising from the cavotricuspid isthmus with saw-tooth morphology on the surface ECG: electrocardiographic and electrophysiologic characteristics. J Interv Card Electrophysiol 2012; 33:127–133.
11. Kistler PM, Sanders P, Hussin A, et al. Focal atrial tachycardia arising from the mitral annulus: electrocardiographic and electrophysiologic characterization. J Am Coll Cardiol 2003;41:2212–2219.
12. Ouyang F, Ma J, Ho SY, et al. Focal atrial tachycardia originating from the noncoronary aortic sinus: electrophysiological characteristics and catheter ablation. J Am Coll Cardiol 2006;48:122–131.
13. Chen Y, Xia S, Tao Q, et al. Ablation of atrial tachycardia originating from the noncoronary sinus: case report and literature review. J Cardiovasc Med (Hagerstown) 2010;11:389–393.
14. Beukema RJ, Smit JJ, Adiyaman A, et al. Ablation of focal atrial tachycardia from the non-coronary aortic cusp: case series and review of the literature. Europace 2015;17:953–961.
15. Kaneko Y, Kato R, Nakahara S, et al. Characteristics and catheter ablation of focal atrial tachycardia originating from the interatrial septum. Heart Lung Circ 2015; 24:988–995.
16. Guo M, Zhang N, Jia G, et al. A rare focal atrial tachycardia arising from the proximal middle cardiac vein: a case report. BMC Cardiovasc Disord 2023;23:169.
17. Tang CW, Scheinman MM, Van Hare GF, et al. Use of P wave configuration during atrial tachycardia to predict site of origin. J Am Coll Cardiol 1995; 26:1315–1324.
18. Man KC, Chan KK, Kovack P, et al. Spatial resolution of atrial pace mapping as determined by unipolar atrial pacing at adjacent sites. Circulation 1996; 94:1357–1363.
19. Mechulan A, Bun SS, Masse A, et al. An improved window of interest for electroanatomical mapping of atrial tachycardia. J Interv Card Electrophysiol 2022; 63:29–37.